Chem Biol Drug Des 2016; **87:** 213–223

Research Article

Chromanyl–isoxazolidines as Antibacterial agents: Synthesis, Biological Evaluation, Quantitative Structure Activity Relationship, and Molecular Docking Studies

Gagandeep Singh[1], Anuradha Sharma[2], Harpreet Kaur[3] and Mohan Paul S. Ishar[1,*]

[1]Bio-Organic and Photochemistry Laboratory, Department of Pharmaceutical Sciences, Guru Nanak Dev University, Amritsar 143 005, Punjab, India
[2]University Institute of Pharmaceutical Sciences, Panjab University, Chandigarh 160014, India
[3]Department of Microbiology, Guru Nanak Dev University, Amritsar 143 005, Punjab, India
**Corresponding author: Mohan Paul S. Ishar, mpsishar@yahoo.com*

Regio- and stereoselective 1,3-dipolar cycloadditions of *C*-(chrom-4-one-3-yl)-*N*-phenylnitrones (N) with different mono-substituted, disubstituted, and cyclic dipolarophiles were carried out to obtain substituted N-phenyl-3′-(chrom-4-one-3-yl)-isoxazolidines (1-40). All the synthesized compounds were assayed for their *in vitro* antibacterial activity and display significant inhibitory potential; in particular, compound 32 exhibited good inhibitory activity against *Salmonella typhymurium*-1 & *Salmonella typhymurium*-2 with minimum inhibitory concentration value of 1.56 μg/mL and also showed good potential against methicillin-resistant *Staphylococcus aureus* with minimum inhibitory concentration 3.12 μg/mL. Quantitative structure activity relationship investigations with stepwise multiple linear regression analysis and docking simulation studies have been performed for validation of the observed antibacterial potential of the investigated compounds for determination of the most important parameters regulating antibacterial activities.

Key words: 1,3-dipolar cycloaddition, 3-chromanyl–isoxazolidines, ADME properties, antibacterial activity, quantitative structure activity relationship

Received 1 May 2015, revised 27 July 2015 and accepted for publication 30 July 2015

Despite widespread distribution of methicillin-resistant *Staphylococcus aureus* (MRSA), it was initially not considered a major threat due to the availability of vancomycin-related antibiotics that were effective for nearly two decades against serious MRSA infections (1). However, nowadays MRSA has become a serious problem, as the annual mortality attributed to MRSA exceeds that of AIDS in the USA and is considered to be a growing threat to community health (2). The availability of several classes of antibiotics such as oxazolidinones (linezolid) and quinolones (ciprofloxacin) could fill this need; however, most clinical MRSA isolates are sufficiently resistant against these classes, rendering them ineffective in successfully curing many infections (3–14). Hence, the discovery and development of novel antimicrobial agents with optimized pharmacological profile together with increased activity towards resistant strains and with a mode of action different from existing drugs is of considerable interest.

It is well known that introduction of fluorine atom into biologically active substances may lead to improved metabolic stability and consequent pharmacological properties and an increase in therapeutic effect (3–13). Therefore, fluorine atom at 6th position in the fluoroquinolone structure has invariably been associated with improved potency of a range of fluoroquinolones for bacterial infections and enhances the binding affinity to biological targets (14–18). The bio-isosteric equivalence of chromone nucleus and quinolone moiety has been established (19,20). Several fluorine-substituted chromones have been proven to be effective against a variety of biological targets (Figure 1) (3–13,16).

Chromone derivatives possessing heterocyclic substituents at 2 and 3 positions have been reported to possess antiallergic activity, muscular relaxation effect, and (3–13,16) antimicrobial activity. Recently, we had also reported chromanyl–isoxazolidines as apoptosis inducers through the mitochondrial-dependent pathway in HL-60 cells (21).

Based on the above reports on the therapeutic importance of substituted chromones and antimicrobial potential of isoxazolidines (22,23), herein we report the synthesis and antibacterial evaluation of some new derivatives of chromanyl–isoxazolidines for their antibacterial potential. Quantitative structure activity relationship (QSAR) evaluations have been performed to develop the predication models for the identification of lead. The lead molecule was further evaluated using molecular docking studies for better understanding of the crucial interactions of the ligand with the enzyme. This would greatly help to elucidate the probable mode of action and further drug designing/development.

 doi: 10.1111/cbdd.12653

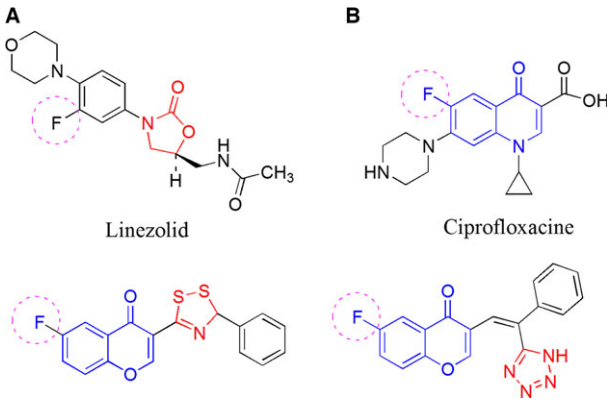

Figure 1: Examples of fluorine-substituted antimicrobial agents.

Methods and Materials

Chemicals

Starting materials and reagents were purchased from commercial suppliers and used after further purification (crystallization/ distillation). ^{1}H- and ^{13}C NMR spectra were recorded at room temperature (30 °C) either on a JEOL (300/75 MHz) NMR spectrometer or a Bruker Advance 500 MHz (500/125 MHz) spectrometer, and chemical shifts (δ) are reported in ppm from tetramethylsilane (TMS) used as the internal standard and coupling constant (J) values in Hertz. IR spectra were recorded on Shimadzu 8400S FT-IR spectrophotometer (KBr, cm^{-1}). Mass spectra, EI, and ESI methods were recorded on Shimadzu GCMS-QP-2000A, Bruker Daltonics Esquire 300 mass spectrometer, and Bruker micrOTOF Q II Mass spectrometer (LC MS/MS). All melting points are uncorrected and measured in open glass-capillaries using Veego Precision Digital Melting Point Apparatus.

General method for synthesis of C-(chromon-3-yl)-N-phenylnitrone (N)

Substituted 3-formylchromone (3.0 g, 2.8 mmol) was dissolved in dry benzene (30 mL), and to the clear solution, *N*-phenyl-hydroxylamine (4.08 g, 2.8 mmol) was added and the contents were slightly heated and allowed to stand at room temperature. After 30 min, *N*-phenylnitrone (N) separated out as a light yellow solid, which was filtered. It was used immediately to prevent its rearrangement.

General procedure for reactions of N-phenylnitrone (5) with various dipolarophiles

Reactions of *N*-phenylnitrones with monosubstituted dipolarophiles were carried out by mixing *N*-phenylnitrone (N, 0.75 mmol) with dipolarophile (2.25 mmol) in dry CH_2Cl_2 (40 mL), and the reaction mixture was stirred under the exclusion of moisture, until all the *N*-phenylnitrone was consumed (TLC). The solvent was removed under vacuum, and the residue was purified by column chromatography using 60–120 mesh silica and 1–8% EtOAc in hexane as eluent. The reactions with disubstituted/cyclic dipolarophile were carried out under the same reaction conditions and products have been isolated by column chromatography. The reported yields were based on isolated pure products and products were characterized by spectroscopic techniques (^{1}H NMR, ^{13}C NMR, IR, and Mass).

5′-acetoxy-2′-phenyl-3′-(6,8-dichloro-chrom-4-one-3yl)-isoxazolidine (11)

Off white semi-solid (86%), **^{1}H NMR** (300 MHz, $CDCl_3$): δ 8.35 (s, 1H, C_2H), 7.96 (bs, 1H, C_5H), 7.37 (dd,,1H, J = 8.5, 5.4 Hz, C_7H), 7.28 (d, 1H, J = 8.5 Hz, C_8H), 7.13-6.81 (m, 5H, Ar-H), 4.77 (dd, 1H, J = 10.2, 5.4 Hz, $C_{5\,\square}$H), 4.42 (dd, 1H, J = 7.8, 2.5 Hz, $C_{3'}$H), 3.13 (dd, 1H, J = 8.7, 6.3 Hz, OCH_2), 2.91 (ddd, 1H, J_{gem} = 12.8 & J = 10.2, 7.8 Hz, $C_{4'}$Ha), 2.62 (ddd, 1H, J_{gem} = 12.8 & J = 5.4, 2.5 Hz, $C_{4'}$Hb); **^{13}C NMR** (75 MHz, $CDCl_3$): δ 175.1, 170.7, 167.8, 149.8, 147.5, 134.3, 129.4, 128.6, 124.2, 124.0, 122.5, 116.3, 114.6, 75.6, 62.9, 52.0, 39.9; **HRMS** (ESI, m/z): calculated for $C_{20}H_{15}Cl_2NO_5$ [M + H]+, 420.0400, found 420.0397.

The compounds (**1**–**40**) were synthesized following the general procedure as described above with the yield of 75–90%.

Biological activity evaluation

In vitro antibacterial studies of all the synthesized compounds (**1**–**40**) were carried out against Gram-negative bacterial strains such as *Salmonella typhymurium*-1 (MTCC-1251) & *Salmonella typhymurium*-2 (MTCC 98) and MRSA (Gram-positive bacterial strain) by disk-diffusion assay. Standard bacterial strains were obtained from Microbial Type Culture Collection (MTCC), Institute of Microbial Technology (IMTECH), Chandigarh, and the clinical isolate methicillin-resistant *Staphylococcus aureus* (MRSA) was obtained from Postgraduate Institute of Medical Education and Research (PGIMER), Chandigarh, India. The activity of compounds was determined in comparison to standard antibiotic discs of gentamicin in triplicate. Prewarmed Mueller-Hinton agar plates were inoculated with 10^6 CFU/mL of test bacteria. Each compound was dissolved in DMSO (1 mg/ml) and then 30 μL of each was pipetted onto sterile paper discs (6 mm diameter) placed on the surface of inoculated agar plates. Plates were incubated at 37 °C for 24 h. Activity was expressed as the diameter of the inhibition zone (mm) produced by the compounds. DMSO was used as negative control. MIC of compounds exhibiting considerable activity was evaluated. The initial optical density (OD) of the medium was measured by spectrophotometer at 600 nm. The test strains were incubated in nutrient broth until the OD reached 0.4–0.6. Then the different concentrations of compounds (0.78, 1.56, 3.12, 6.25, 12.5, 25, 50 μg/mL) were tested

for the inhibition of growth of these microbes, in separate tubes. The 10-mL tubes each containing 5 mL of nutrient broth and 1 mL of different concentrations of compounds were incubated for 24 h with shaking at 180 rpm using a rotary shaker. Each tube corresponding to different concentrations was observed and concentration showing apparently no turbidity was considered to be the MIC of the respective compound.

Quantitative structure–activity relationship

QSAR analysis applies statistical methods to describe the relationship between chemical structure and biological activities of a series of chromanyl isoxazolidines quantitatively. The groups of calculated thermodynamic descriptors included bend energy, heat of formation, torsion energy, boiling point, melting point, Gibbs free energy, Henry's law constant, ideal gas thermal capacity, exact mass, and molecular weight. Steric descriptors derived were steric energy, connolly accessible area, connolly molecular area, connolly solvent excluded volume, molar refractivity, and ovality; apart from this partition coefficient calculated as LogP. Electronic descriptors include kinetic energy, potential energy, and total energy. Molecular topology descriptors included balaban index, cluster count, molecular topological index, num rotatable bonds, polar surface area, radius, shape attribute, sum of degrees, sum of valence degrees, topological diameter, total connectivity, total valence connectivity, and Wiener index.

Molecular docking study

The comparative and automated docking studies were performed using GRID-based ligand docking with energetics (GLIDE) program (version 6.3, Schrodinger, LLC, New York, NY, USA) to determine the best *in silico* conformation of synthesized molecule inside the active site. The standard drugs such as ciprofloxacin and linezolid were drawn and docked back into the protein in order to determine the reliability of the docking method. The crystal structure of the topo II DNA gyrase with its co-crystal ciprofloxacine (PDB ID: 2XCT) was selected as target, to understand the nature of the interaction between the most potent molecule and DNA gyrase. All the ligand molecules were designed and the structures were analyzed using ChemDraw Ultra 10 3D. The minimization of ligands and protein was performed by universal force field and amber force field respectively. Binding site was defined by the selecting the active amino acids of the enzyme structure and the grid with its dimensions (51 × 53 × 46) were defined.

Physicochemical and ADME properties

ADME properties were calculated using QIKPROP v3. 6 tool of Schrodinger Software. It predicts both physicochemically significant descriptors and pharmacokinetically significant properties. QIKPROP provides ranges for comparing a exacting molecule's properties with those of 95% of known drugs. QIKPROP also flags 30 types of reactive functional groups that may cause false positives in high throughput screening (HTS) assays. It also evaluates the suitability of analogs based on Lipinski's rule of five, which is essential to ensure drug like pharmacokinetic profile while using rational drug design. All the analogs were neutralized before being used by QIKPROP.

Results and Discussion

Chemistry

The *C*-(chrom-4-one-3-yl)-*N*-phenylnitrones (**N**) were prepared in good yields by reacting various substituted 3-formylchromones and *N*-phenylhydroxylamine (1 molar equivalent) in dry benzene with constant stirring, followed by removal of the solvent under vacuum (24). The synthesized nitrones were reacted with various monosubstituted dipolarophiles by stirring in dry dichloromethane at room temperature leading to isoxazolidines (**1-29**, Scheme 1) (21,24).

Further, the synthesized nitrones (**N**) were reacted with disubstituted and cyclic dipolarophiles, under similar set of conditions to obtain isoxazolidines (**30**-**40**) (21). All the products were separated and purified by column chromatography and characterized by modern spectroscopic techniques, that is, ^{1}H & ^{13}C NMR and Mass (Scheme 2).

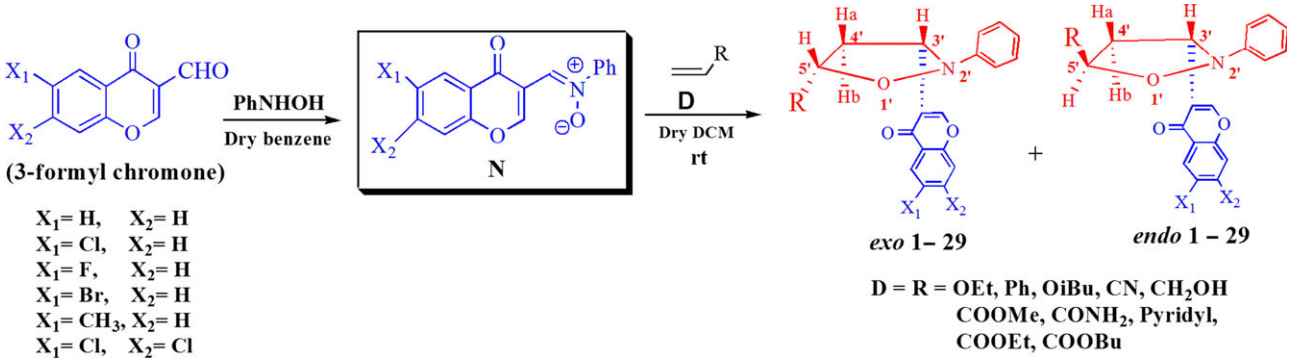

Scheme 1: Reaction of various nitrones (**N**) with monosubstituted dipolarophiles leads to chromanyl-isoxazolidines (**1–29**).

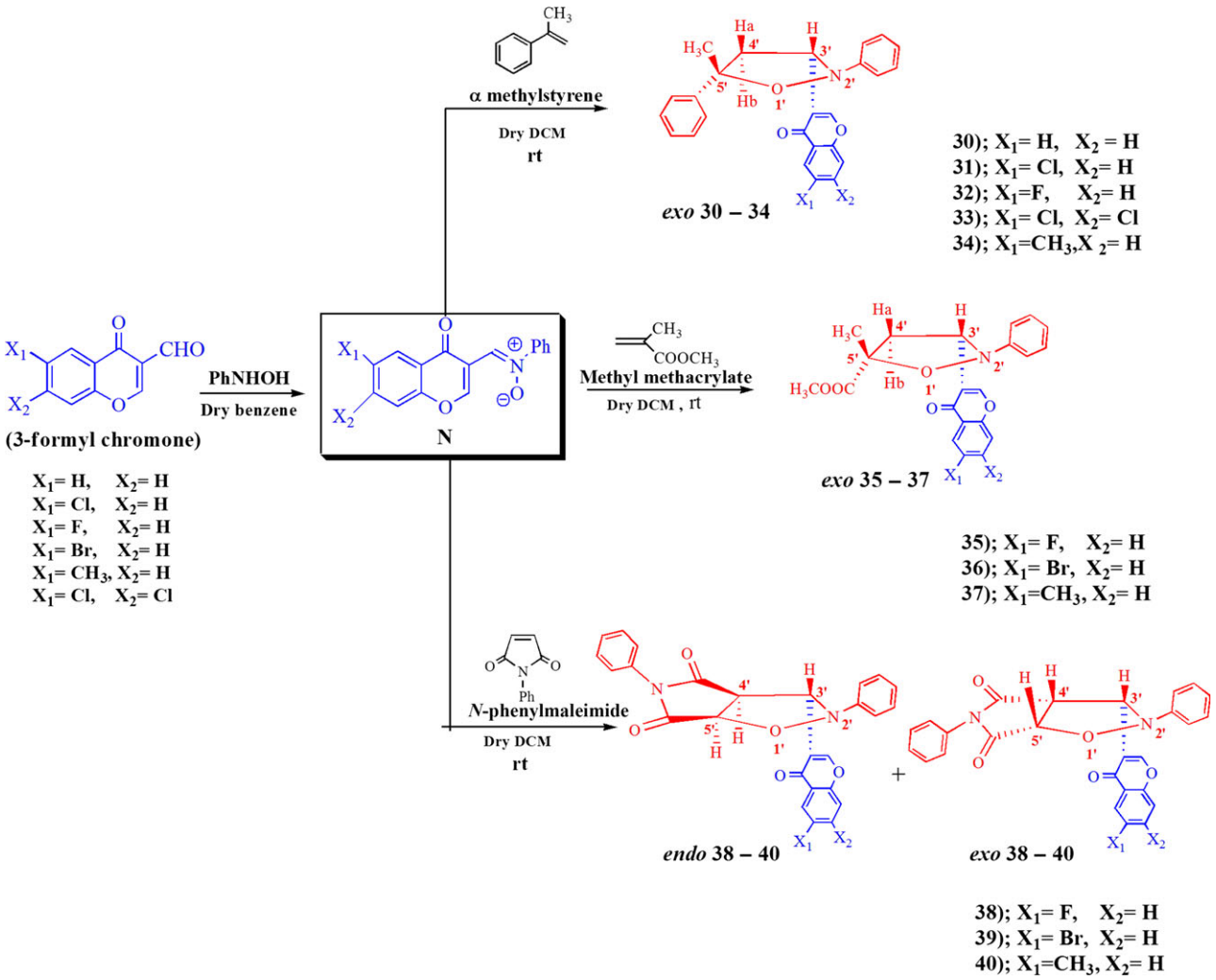

Scheme 2: Reaction of various nitrones (**N**) with disubstituted and cyclic dipolarophile.

Antibacterial activity

In vitro antibacterial studies of all the synthesized compounds (**1-40**) were carried out against Gram-negative bacterial strains such as *Salmonella typhymurium*-1 (MTCC-1251) & *Salmonella typhymurium*-2 (MTCC 98) and Gram-positive strain such as MRSA bacterial strain by disk-diffusion assay (25). The activity of compounds was determined in comparison with standard antibiotic disks of Gentamycin. Minimum inhibitory concentration (MIC) of compounds exhibiting considerable activity (Table 1) was determined using serial dilution method (26). The initial optical density (OD) of the medium was measured by spectrophotometer at 600 nm.

All the synthesized chromanyl–isoxazolidine derivatives exhibit good to moderate antibacterial activity with observable variations due to different substitutions at C5′ and C6. The obtained results revealed that some of the compounds possess excellent antibacterial activity against selected strains. Among the evaluated molecules, disubstituted and bicyclic isoxazolidines displayed much higher inhibitory potential against *S. typhi* 1 & *S. typhi* 2 than positive control, that is, Gentamycin. In particular, compound **32** exhibited good inhibitory activity against *S. typhi* 1 & *S. typhi* 2 with MIC value of 1.56 μg/mL and also showed good potential against MRSA with MIC of 3.12 μg/mL.

In the case of monosubstituted isoxazolidines, compounds bearing non-polar hydrophobic groups at C5′ show good to moderate antibacterial activity. For instance compounds such as **11, 15, 18,** and **22** display significant antibacterial activities with MIC value of 6.25, 3.12, 3.12, and 6.25 μg/mL, respectively, against *S. typhi* 1. Similarly, compounds **3, 6,** and **25** bearing ethoxy, isobutoxy, and phenyl at C5′ and fluoro substitution at C6 showed good inhibitory activity with MIC value of 12.5, 12.5, and 3.12 μg/mL, respectively, against *S. typhi* 1. The inhibitory potential difference in compound **3, 6,** and **25** can be attributed to the difference in the hydrophobic character of ethoxy/isobutoxy/

Table 1: *In vitro* antibacterial activity of synthesized compounds **1**–**40** against various bacterial strains

	Nitrone			MIC (μg/mL)		
Comp. No.	X_1	X_2	Dipolarophile	*Salmonella typhymurium*-1	*Salmonella typhymurium*-2	MRSA
1	H	H	**D**; R = -OEt	25	25	25
2	CH_3	H	R = -OEt	25	25	25
3	F	H	R = -OEt	12.5	12.5	25
4	Br	H	R = -OEt	25	25	25
5	Cl	Cl	R = -OEt	25	25	25
6	F	H	R = -OiBu	12.5	25	25
7	Br	H	R = -OiBu	25	25	25
8	CH_3	H	R = -OiBu	25	25	25
9	H	H	R = -CO_2Me	25	25	25
10	Cl	H	R = -CO_2Me	12.5	12.5	25
11	Cl	Cl	R = -CO_2Me	6.25	6.25	25
12	H	H	R = -$CONH_2$	12.5	12.5	25
13	Cl	H	R = -CN	6.25	6.25	25
14	H	H	R = -CH_2OH	12.5	12.5	25
15	Cl	Cl	R = -CH_2OH	3.12	12.5	25
16	H	H	R = -CO_2Et	12.5	12.5	25
17	Cl	H	R = -CO_2Et	6.25	12.5	25
18	F	H	R = -CO_2Et	3.12	6.25	12.5
19	CH_3	H	R = -CO_2Et	25	25	25
20	H	H	R = -CO_2Bu	25	25	25
21	Cl	H	R = -CO_2Bu	12.5	12.5	25
22	F	H	R = -CO_2Bu	6.25	6.25	12.5
23	CH_3	H	R = -CO_2Bu	25	25	25
24	H	H	R = -Ph	25	25	25
25	F	H	R = -Ph	3.12	6.25	25
26	Br	H	R = -Ph	12.5	12.5	25
27	Cl	Cl	R = -Ph	6.25	6.25	25
28	CH_3	H	R = -Ph	25	25	25
29	H	H	R = -Pyridyl	6.25	6.25	25
30	H	H	α-Me-Styrene	12.5	12.5	25
31	Cl	H	α-Me-Styrene	6.25	6.25	25
32	F	H	α-Me-Styrene	1.56	1.56	3.12
33	Cl	Cl	α-Me-Styrene	6.25	6.25	25
34	CH_3	H	α-Me-Styrene	12.5	12.5	25
35	F	H	Methyl methacrylate	6.25	12.5	25
36	Br	H	Methyl methacrylate	25	25	25
37	CH_3	H	Methyl methacrylate	25	25	25
38	F	H	*N*-Ph-maleimide	3.12	6.25	25
39	Br	H	*N*-Ph-maleimide	25	25	25
40	CH_3	H	*N*-Ph-maleimide	25	25	25
Gentamycin				1.56	1.56	0.39

MIC, minimum inhibitory concentration; MRSA, methicillin-resistant *Staphylococcus aureus.*

phenyl at C5′. Compound **25** also displayed significant antibacterial activity against *S. typhi* 2 with MIC value of 6.25 μg/mL. Both strains *S. typhi* 1 & *S. typhi* 2 displayed sensitivity against compound **29** bearing pyridyl at C5′ with MIC value 6.25 μg/mL (Table 1).

Furthermore, in the case of disubstituted and bicyclic isoxazolidines, compounds **31** and **32** showed good antibacterial activity against *S. typhi* 1 and *S. typhi* 2 with MIC value of 6.25 and 1.56 μg/mL, respectively. It is widely accepted that one or just a few atoms in an organic molecule can dramatically alter its chemical and biological nature, including its potency, stability, lipophilicity, and bioavailability (17,18). Thus, difference in inhibitory potential of compounds **32** and **31** may be attributed to the presence of fluoro- and chloro- groups at C6. Compound **32**, a fluorinated analog also displays significant inhibitory potential against MRSA with MIC value of 3.12 μg/mL. Among bicyclic isoxazolidines, compound **38** showed good inhibition against *S. typhi* 1 (MIC = 3.12 μg/mL).

Among the various halogens at C6, fluoro substitution shows distinct enhancement in the activity against all the tested bacterial strains. Thus, all fluoro-substituted compounds such as **3**, **6**, **18**, **22**, **25**, **32**, **35,** and **38** exhibited significant antibacterial activities against *S. typhi* 1, *S. typhi*

2, and MRSA strains in comparison with other analogs. This influence of flouro- on enhancement of antibacterial activity is reminiscent of significance of fluoro substitution at an identical position in antibacterial activity of fluoroquinolone class of compounds such as norfloxacin, ofloxacin, ciprofloxacin etc., wherein fluoro substituent is shown to improve the DNA gyrase inhibition up to 15- to 18-fold over its 6-hydrogen analog (18).

Quantitative structure activity relationship

Quantitative structure activity relationship investigations have been carried out to describe the relationship between chemical structure and biological activities of a series of chromanyl–isoxazolidines (**1**-**40**). Various thermodynamic, electronic, steric, and molecular topology descriptors have been calculated using CHEMDRAW 12 (Cambridge Soft Corporation, Cambridge, MA, USA).

As no outliers were identified, therefore, it is important to note that all these models were developed using the entire set (n = 40). For the generation of models, the entire data set was divided into training (n = 30) and test set (n = 10) by K-means of clustering (Table S1). The whole data were divided into four subgroups from each of which 25% of compounds were selected as the members of the test set (Table S2). Stepwise multiple linear regression analysis method was employed to generate QSAR using MINITAB software (27), and its validation was carried out by leave-one-out (LOO) cross-validation method. The quality of the model is indicated by the various parameters such as correlation coefficient (r), Fisher's statistics (F), standard error of estimation (s), and adjusted coefficient of variation (r^2_{adj}).

A number of QSAR models were developed using all the generated descriptors as independent variables for the compounds against the *S. typhi 1* and *S. typhi 2*. Out of all, best two models (M-1 and M-2) were shown for the in-depth understanding of the crucial factors required for the activity.

$$\begin{aligned} pMIC_{50} = {} & 2.278 + 0.143\,(\text{Shape Attribute}) \\ & - 0.0087\,(\text{Connolly Molecular Area}) \\ & - 0.110\,(\text{Mol Refractivity}) \\ & - 0.099\,(\text{Henry's Law Constant}) \\ & + 0.251\,(\text{Topological Diameter}) \\ & + 8873\,(\text{Total Connectivity}) \end{aligned} \quad \text{(M-1)}$$

r^2 = 77.40, r^2 (adj) = 71.50, r^2 (pred) = 65.42, q^2 = 74.39.

In model M-1, consensus of five type of descriptors was found to be very significant for forecasting the biological activity. The inhibitory activity is directly proportional to the shape attribute, topological diameter, and total connectivity as evidenced by the positive regression coefficient. This model shows large negative correlation of the steric parameter connolly molecular area and Henry's law constant. The physicochemical parameter such as molecular refractivity is combination of steric bulk (volume) and polarizability of the substituents. A smaller MR indicates the strong interactions within the enzyme and good possibility in drug-receptor interactions. A negative correlation suggests that a high polarizability is not desirable for the good activity. The topological diameter has favorable contribution as evidenced by positive regression coefficient. It can be clearly understood in the case of compounds **32**, **33**, **34**, **35**, **36,** and **37** that more the topological diameter, greater will be inhibitory concentration. Partition coefficient (LogP), number of rotatable bonds, and Gibbs free energy have an unfavorable contribution toward the binding inhibitory activity.

The model proved to be robust and reliable as shown from the values s = 0.608, r^2 = 0.774, r^2 (adj) = 0.715, PRESS = 1.01, pred_r^2 = 0.654, and q^2 = 0.743 which are much satisfactory than the stipulated value of 0.5. The predictive potential of this model was determined by q^2 of the test set compounds, and it was found to be 74.3% (Figure 2A,B).

The model **M-2** is developed against *S. typhi* 2 for the explanation of structure activity relationship.

$$\begin{aligned} pMIC_{50} = {} & 5.332 + 0.00173\,(\text{Critical Volume}) \\ & - 0.158\,(\text{Shape Attribute}) \\ & - 0.0156\,(\text{Ideal Gas Thermal Capacity}) \\ & - 0.099\,(\text{Num Rotatable Bonds}) \\ & - 0.071\,(\text{Mol Refractivity}) \\ & + 0.048\,(\text{Henry's Law Constant}) \end{aligned} \quad \text{(M-2)}$$

r^2 = 71.35, r^2 (adj) = 63.87, r^2 (pred) = 54.20, q^2 = 73.29.

In this model **M-2**, all the found descriptors have favorable contribution toward enzyme inhibition except ideal gas thermal capacity and molecular refractivity. Ideal gas ther-

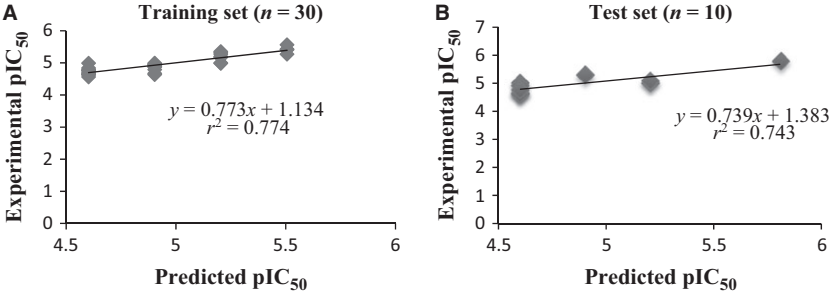

Figure 2: Correlation between observed and calculated/predicted activity using model 1 [**M1**] for (A) Training Set and (B) Test Set.

mal capacity and critical pressure should be less to exhibit higher activity as evidenced by negative regression coefficient. These findings suggest that the attenuation of these parameters will lead to enhance inhibitory activity. Molecular refractivity is indirectly proportional to the inhibitory activity. As fluorine has less molecular refractivity than chlorine so that compound **32** is more potent than compound **31.** Compounds **31** and **32** showed good antibacterial activity against *S. typhi* 1 & *S. typhi* 2 with MIC = 6.25 and 1.56 μg/mL, respectively. The difference in the inhibitory activity of the compounds **32** and **31** attributed to the presence of fluoro- and chloro- group, respectively, at C6 position is due to the higher polar surface area of the former. The quality of fit was justified by the correlation graphs as shown in the Figure 3. The model proved to be reliable and statistically significant as the value of r^2 and r^2 (pred) is 71.35 and 54.20, respectively.

Based on these models, it is observed that the predicted antibacterial activities by our QSAR models were very close to those experimentally observed, indicating that these models can be safely applied for forecasting of more effective hits having the same skeletal framework.

Molecular docking studies

Considering the potent activity of synthesized compounds (**1**–**40**) as new antibacterial agents observed in *in vitro* study, it was worthwhile to perform molecular docking studies (*in silico* virtual screening), to support the *in vitro* activity and to determine the best *in silico* conformation of most potent molecule. In our research group, the bio-isosteric equivalence of chromone nucleus and quinolone moiety has been established (19,20), and it is pertinent to mention here that the chromone analogs may follow same mode of action as of various fluoroquinolones such as ciprofloxacin and norfloxacin, by inhibiting DNA gyrase; therefore, the crystal structure of the topo II DNA gyrase with its cocrystal ciprofloxacin (PDB ID: 2XCT) was selected as target, to understand the nature of the interaction between the most potent molecule and DNA gyrase (28). DNA gyrase, a type II topoisomerase responsible for DNA replication and repair, is essential in all bacteria and absent in eukaryotes (29). The enzyme catalyzes the interconversion of various topological forms of DNA, an essential process in DNA replication. The crystal structure of topoisomerase II DNA gyrase with its cocrystal surrounding by active amino acids is shown in Figure 4.

The comparative and automated docking studies were performed using GLIDE program to determine the best *in silico* conformation of synthesized molecule inside the active site (30). The standard drugs such as ciprofloxacin and linezolid were drawn and docked back into the protein to determine the reliability of the docking method. Figure 5 clearly shows the important interactions of the both standard drugs in the enzyme pocket.

The predicted binding interactions were analyzed, and the hypothetical binding mode of all the ligands in the defined

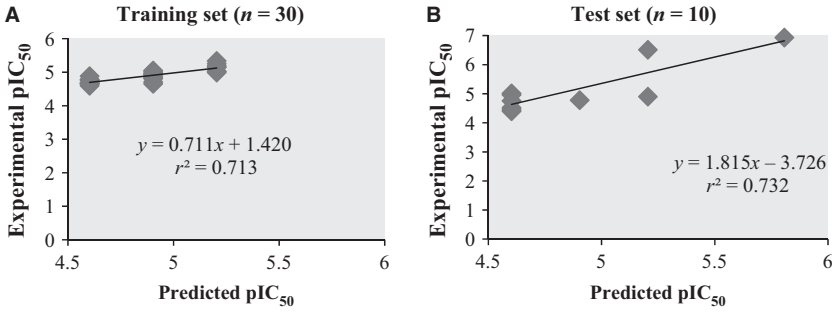

Figure 3: Correlation between observed and calculated/predicted activity using model **M4** for (A) Training Set and (B) Test Set.

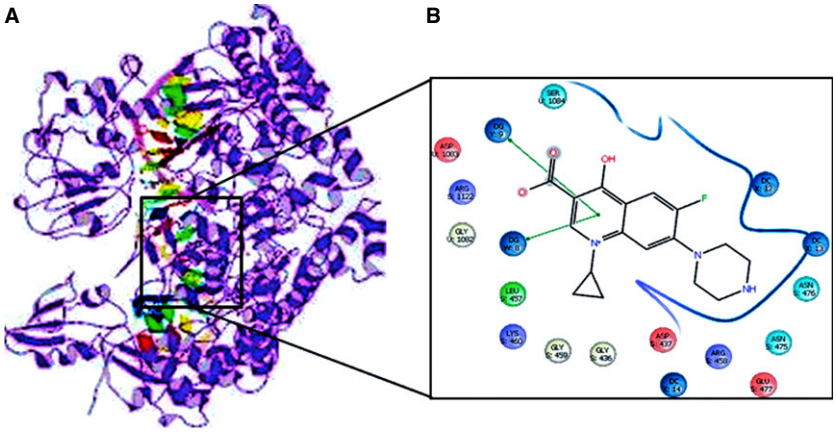

Figure 4: (A) The crystal structure of topoisomerase II DNA gyrase with its cocrystal found by site-map. (B) Active amino acids surrounding the cocrystal in the binding pocket.

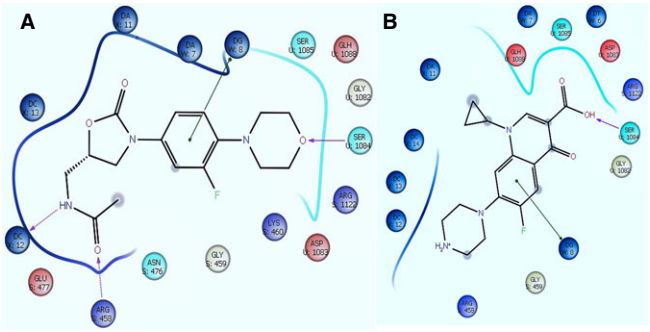

Figure 5: (A) Hypothetical binding orientation showing the important interactions of the **linezolid** and (B) **ciprofloxacin** in the enzyme pocket (2D-VIEW).

grid of the crystal structure is shown in the Figure 6. Theoretically, all the synthesized compounds showed G score ranging from −7.68 to −3.31 (Table S3).

Among the series, docking of DNA gyrase enzyme with **32** revealed that its dock score (−7.68) was quite comparable with standard drug ciprofloxacin (dock score −6.37). The docking binding model of compound **32** indicated that it was well filled in the active site. The docked compound **32** formed hydrogen bonding with GLH 1088 and π–π interaction with DG 8 (Figure 7).

Another moderately active compound **33** also shows hydrogen bonding with GLH-1088; however, there is no pie–pie interaction with any amino acids (Figure 8). Therefore, the activity may be attributed to inhibition of enzyme DNA gyrase, which is crucial for the essential processes of DNA transcription and cell replication.

Physicochemical and ADME properties

On account of unfavorable absorption, distribution, metabolism, and elimination (ADME) parameters, most of

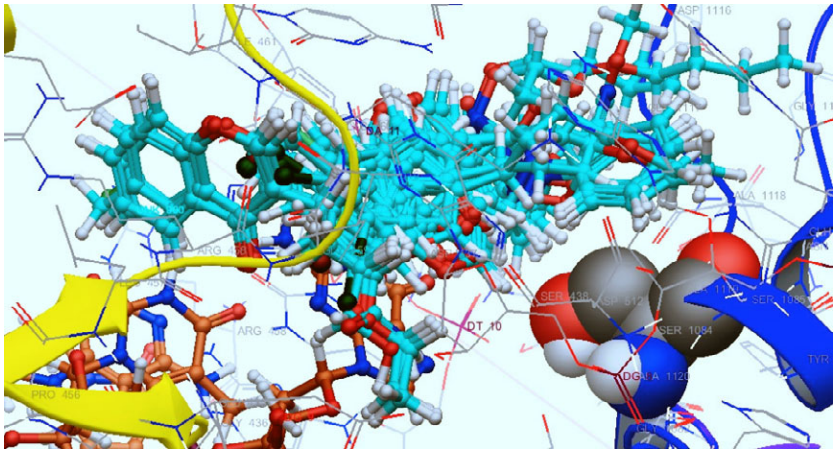

Figure 6: Binding orientation of all ligands in the binding pocket of the enzyme structure.

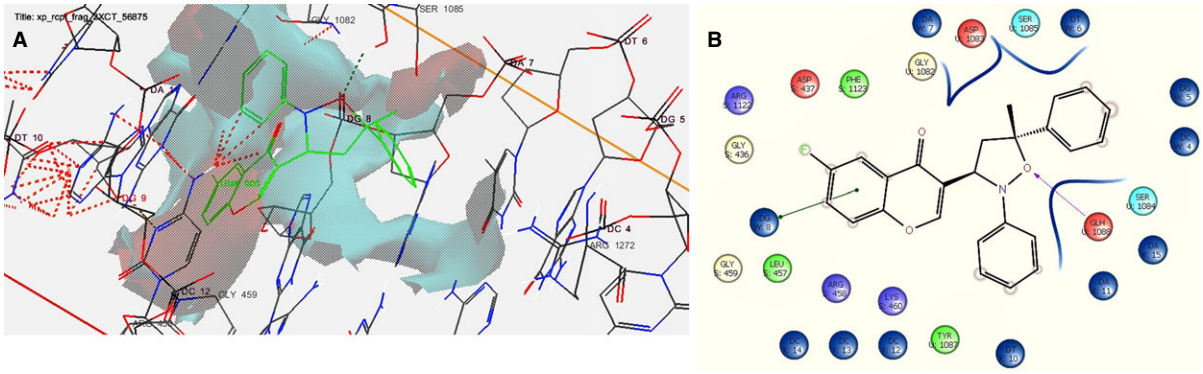

Figure 7: (A) Binding orientation of the active compound **32** in the enzyme pocket showing hydrophilic (blue colored) and hydrophobic map (brown colored). (B) Another pose of the same compound showing pie–pie interactions with **DG 8** and hydrogen bonding interactions with **GLH 1088** (2D view).

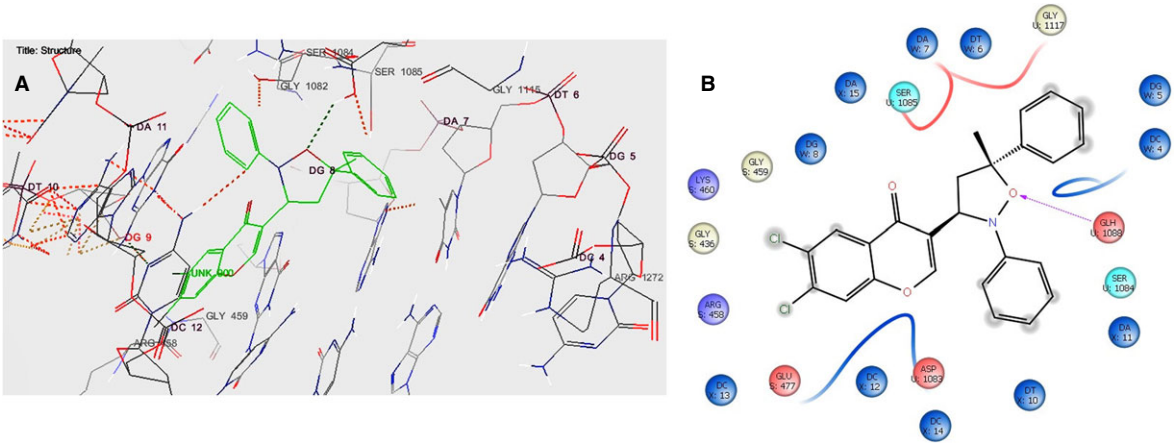

Figure 8: (A) Hypothetical mode of compound **33** forming the hydrogen bond with **GLH 1088** in the binding pocket of the enzyme. (B) In the case of moderate active compound **33**, there is no formation of pie–pie interactions (2D view).

the potential therapeutic agents fail to reach the clinic. Therefore, a computational study of synthesized compounds **1**–**40** was performed using QIKPROP v3.6 tool of Schrodinger software for the assessment of ADME properties, and values obtained are depicted in Table 2b. From all these parameters, it can be observed that compound **32** exhibits significant ADME properties in the acceptable range.

A molecule likely to be developed as an orally active drug candidate should show no more than one violation of the following four criteria: number of hydrogen bond acceptor ≤10, number of hydrogen bond donor ≤5, logP (octanol–water partition coefficient) ≤5, and molecular weight ≤500. All the synthesized molecules showed significant values for the ADME properties analyzed (Table S4) and exhibited drug-like characteristics based on Lipinski's rule of 5;(31) therefore, these compounds can be further developed as oral drug candidates.

Conclusion

Based on our previous work, we have synthesized series of chromanyl–isoxazolidines (**1-40)**, evaluated for their antibacterial activity against *S. typhi* 1, *S. typhi* 2, and MRSA bacterial strains. All the fluorine-substituted analogs showed significant antibacterial activities in comparison with other analogs. In particular, compound **32**, having fluoro substituent at C6 was found to have the most potent inhibitory potential against *S. typhi*-1, *S. typhi*-2, and methicillin-resistant *Staphylococcus aureus*, which also points toward possibly an identical mode of action as fluoroquinolones; supported by docking analysis. Correlation of the results obtained from docking and QSAR studies provides information of structural requirements for the enhanced activity. It can be used in rationalization of the activity trends in the molecules under study. Therefore, our findings support that disubstituted (**30**–**34**) and bicyclic (**38-40**) isoxazolidines have promising potential as lead compounds for the design of new antibacterial agent.

Acknowledgments

Financial support from CSIR, New Delhi (02(0082)/12/EMR-II) to GS is gratefully acknowledged. UGC, New Delhi, is acknowledged for grant to G.N.D.U. Amritsar under UPE program.

Conflict of interest

The authors declare they have no conflict of interests.

Table 2: *In silico* predicted ADME properties for good oral bioavailability of potent compound **32**

	Predicted physicochemical pharmacokinetic properties								
Entry	n-ON acceptors	n-OHNH donors	nROTB	PSA (Å^2)	QP logP	QP logS	QP logK	QP logBB	MW
Comp.32	4	0	3	43.10	5.683	−6.651	−0.332	0.405	401.43

n-ON acceptors: number of H-bond acceptors; n-OHNH donors: number of H-bond donors; nROTB: number of rotatable bonds; PSA: polar surface area; QP logP: predicted octanol/water partition coefficient; QP logS: predicted aqueous solubility; QP logK: prediction of binding to human serum albumin; QP logBB: prediction of Blood/Brain partition coefficient; MW: molecular weight; ADME, absorption, distribution, metabolism, and elimination.

References

1. Veale C.G.L., Zoraghi R., Young R.M., Morrison J.P., Pretheeban M., Lobb K.A., Reiner N.E., Andersen R.J., Davies-Coleman M.T. (2015) Synthetic analogues of the marine bisindole deoxytopsentin: potent selective inhibitors of MRSA pyruvate kinase. J Nat Prod;78:355–362.
2. Michalska K., Karpiuk I., Krol M., Tyski S. (2013) Recent development of potent analogues of oxazolidinone antibacterial agents. Bioorg Med Chem;21:577–591.
3. Diwakar S.D., Bhagwat S.S., Shingare M.S., Gill C.H. (2008) Substituted 3-((*Z*)-2-(4-nitrophenyl)-2-(1H-tetrazol-5-yl) vinyl)-4H-chromen-4-ones as novel anti-MRSA agents: synthesis, SAR and in-vitro assessment. Bioorg Med Chem Lett;18:4678–4681.
4. Filler R., Kobayashi Y. (1982) Biomedicinal Aspects of Fluorine Chemistry. Tokyo and Amsterdam: Kodansya and Elsevier Biomedical.
5. Welch J.T., Eswarakrishman S. (1991) Fluorine in Bioorganic Chemistry. New York: JohnWiley & Sons.
6. Filler R., Kobayashi Y., Yagupolskii L.M. (1993) Organofluorine Compounds in Medicinal Chemistry and Biomedical Applications. Amsterdam: Elsevier.
7. Kukhar V.P., Soloshonok V.A. (1995) Fluorine Containing Amino Acids: Synthesis and Properties. Chichester: John Wiley & Sons Ltd.
8. Ojima I., McCarthy J.R., Welch J.T. (1996) Biomedical Frontiers of Fluorine Chemistry. Washington, D.C.: American Chemical Society.
9. Hiyama T. (2000) Organofluorine Compounds, Chemistry and Applications. Berlin: Springer.
10. Kirsch P. (2004) Modern Fluoroorganic Chemistry. Weinheim: Wiley-VCH Verlag GmbH.
11. Uneyama K. (2006) Organofluorine Chemistry. Oxford: Blackwell.
12. Begue J-P., Bonnet-Delpon D. (2006) Recent advances (1995–2005) in fluorinated pharmaceuticals based on natural products. J Fluor Chem;127:992–1012.
13. Kirk K.L. (2006) Fluorine in medicinal chemistry: recent therapeutic applications of fluorinated small molecules. J Fluor Chem;127:1013–1029.
14. Kim H.Y., Wiles J.A., Wang Q., Pais G.C.G., Lucien E., Hashimoto A., Nelson D.M., Thanassi J.A., Podos S.D., Deshpande M., Pucci M.J., Bradbury B.J. (2011) Exploration of the activity of 7-Pyrrolidino-8-methoxy-isothiazoloquinolones against methicillin-resistant *Staphylococcus aureus* (MRSA). J Med Chem;54:3268–3282.
15. Barbachyn M.R., Cleek G.J., Dolak L.A., Garmon S.A., Morris J., Seest E.P., Thomas R.C., *et al.* (2003) Identification of phenylisoxazolines as novel and viable antibacterial agents active against gram-positive pathogens. J Med Chem;46:284–302.
16. Raj T., Bhatia R.K., Sharma R.K., Gupta V., Sharma D., Ishar M.P.S. (2009) Mechanism of unusual formation of 3-(5-phenyl-3H-[1,2,4]dithiazol-3-yl)chromen-4-ones and 4-oxo-4H-chromene-3-carbothioic acid *N*-phenylamides and their antimicrobial evaluation. Eur J Med Chem;44:3209–3216.
17. Alaa A.M., Abdel A., Yousif A.A., Mohamed H.M.A. (2011) Design, synthesis and antibacterial activity of fluoroquinolones containing bulky arenesulfonyl fragment: 2D-QSAR and docking study. Eur J Med Chem;46:5487–5497.
18. Domagala J.M., Hanna L.D., Heifetz C.L., Hutt M.P., Mich T.F., Sanchez J.P., Solomon M. (1986) New structure activity relationships of the quinolone antibacterials using the target enzyme. The development and application of a DNA gyrase assay. J Med Chem;29:394–404.
19. Ishar M.P.S., Singh G., Singh S., Sreenivasan K.K., Singh G. (2006) Design, synthesis, and evaluation of novel 6-chloro-/fluorochromone derivatives as potential topoisomerase inhibitor anticancer agents. Bioorg Med Chem Lett;16:1366–1370.
20. Mayer C., Janin Y.L. (2014) Non-quinolone inhibitors of bacterial type-IIA topoisomerases: a feat of bioisosterism. Chem Rev;114:2313–2342.
21. Singh G., Kaur A., Sharma V., Suri N., Sharma P.R., Saxena A.K., Ishar M.P.S. (2013) Synthesis and cytotoxicity evaluation of regioisomeric substituted *N*-phenyl-3′-(chrom-4-one-3-yl)-isoxazolidines: induction of apoptosis through a mitochondrial-dependent pathway. Medchemcommun;4:972–978.
22. Keri R.S., Budagumpi S., Pai R.K., Balakrishna R.G. (2014) Chromones as a privileged scaffold in drug discovery: a review. Eur J Med Chem;78:340–374.
23. Chakraborty B., Samanta A., Sharma P.K., Chhetri M.S., Kafley S., Banerjee A., Sinha C. (2010) One pot high yield synthesis of some novel isoxazolidine derivatives using *N*-methyl-α-chloro nitrone in water and their antibacterial activity. J Chem Pharm Res;2:727–739.
24. Ishar M.P.S., Singh G., Kumar K., Singh R. (2000) Investigations on peri-, regio- and stereoselectivities in thermal cycloadditions involving C-(4-Oxo-4H[1]benzopyran-3-yl)-N-phenylnitrones: role of steric factors and secondary interactions in 1,3-dipolar cycloadditions. Tetrahedron;56:7817–7828.
25. Mitic-Culafic D., Vukovic-Gacic B., Knezevic-Vukcevic J., Stankovic S., Simic D. (2005) Comparative study on the antibacterial activity of volatiles from sage (Salvia officinalis L.). Arch Biol Sci;57:173–178.
26. Hindler J., Mahon C.C., Manuselis G. (1995) Textbook of Diagnostic Microbiology Special Antimicrobial Susceptibility Tests. China: Saunders Elsevier; 89.
27. Darlington R.B. (1990) Regression and Linear Models. New York: McGraw-Hill.
28. Bax B.D., Chan P.F., Eggleston D.S., Fosberry A., Gentry D.R., Gorrec F., Giordano I., *et al*. (2010) Type IIA topoisomerase inhibition by a new class of antibacterial agents. Nature;466:935–940.
29. Hameed S., Raichurkar A., Madhavapeddi P., Menasinakai S., Sharma S., Kaur P., Nandishaiah R., Pan-

duga V., Reddy J., Sambandamurthy V.K., Sriram D. (2014) Benzimidazoles: novel mycobacterial gyrase inhibitors from scaffold morphing. ACS Med Chem Lett;5:820–825.
30. Halgren T.A., Murphy R.B., Friesner R.A., Beard H.S., Frye L.L., Pollard W.T., Banks J.L. (2004) Glide: a new approach for rapid, accurate docking and scoring. 2. Enrichment factors in database screening. J Med Chem;47:1750–1759.
31. Lipinski C.A., Lombardo F., Dominy B.W., Feeney P.J. (2012) Experimental and computational approaches to estimate solubility and permeability in drug discovery and development settings. Adv Drug Deliv Rev;64:4–17.

Notes

[a]Small-Molecule Drug Discovery Suite 2014-2: Glide, version 6.3, Schrödinger, LLC, New York, NY, 2014.
[b]Schrodinger, LLC. New York, USA: Schrodinger Inc.; 2008

Supporting Information

Additional Supporting Information may be found in the online version of this article:

Table S1. Training set (*n* = 30) and test set (*n* = 10) ligands obtained through K-Means clustering.

Table S2. K-Means clustering of ligands (*n* = 40) using calculated descriptors.

Table S3. Dock Score for all the synthesized compounds (**1–40**).

Table S4. *In silico* predicted ADME properties for good oral bioavailability of compounds **1–40**.